Study of possibilities of getting nanocarbons from butadien-1.3 and texture characteristics of nanocarbons and catalyses

Sherali Djanikulov[1], and *Normurot* Fayzullayev[2*]

[1]Military-academic lyceum"Temurbeklar maktabi" in Shakhrisabz, Uzbekistan
[2]Samarkand State University, Samarkand, Uzbekistan

Abstract. The purpose of the study is to study the possibility of obtaining nanocarbons in a catalyst containing 15%Ni*5%Co*5%Fe*5%Cu*2% Mo/HSZ and to check the texture characteristics of the catalyst and nanocarbon. The research method is a catalyst containing 15%Ni*5%Co*5%Fe*5%Cu*2%Mo/HSZ prepared by precipitation of nitrates of the corresponding metals. The method of examination is electron microscopy. The morphological composition of the samples was performed by scanning electron microscopy (SEM) on a device "JEOL JSM-6390 LA" equipped with an energy dispersion X-ray microanalysis unit (EDX). We place the sample on double-sided carbon conductive tape glued to a copper-chrome table. Then we vacuum it in the instrument chamber. Microphotography recording was performed at 5-25 kV working distances and 8-10 mm under accelerating voltage. EDX spectra were recorded at 20 kV, with a working distance of 10 mm. The microstructure of the samples was examined by scanning electron microscopy. The JEOL 2100F used an accelerating voltage of 200 kV. The samples were dispersed, processed in ultrasound with methanol, and rubbed on a copper wall. The catalysts were preheated and passivated at 400 °C for 4 h at a 30 ml/min flow of nitrogen. Recycled catalysts are also 2% by volume in an oxygen-argon mixture. The O_2/Ar reaction was inactivated at room temperature after cessation. The average size of the metal particles and the diameter of the carbon nanotubes were determined in the Image-ProPlus program. We calculated the average size of 500 particles for each catalyst, and 100 carbon nanotubes were processed to measure the average diameter of the carbon nanotubes. After synthesis and functionalization of carriers in the catalyst 15%Ni*5%Co*5%Fe*5%Cu*2%Mo/HSZ, the nanocarbons were condensed, and their outer diameter remained unchanged and amounted to 10-30 nm. Carbon nanotubes range in diameter from 5 to 15 nm, depending on the size of the metal particles, and in length from a few microns. The main conclusions are that the highly dispersed metal particles located at the ends of the nanotubes are an important factor in the growth of nanotubes. Larger iron particles are characterized by changes in the diameter of carbon nanotubes during growth. At the beginning of growth, the diameter of such a nanotube is 30...50 nm; however, it decreases to 5...15 nm.

*Corresponding author: fayzullayev72@inbox.ru

1 Introduction

Carbon materials are very diverse and are widely used in a variety of industries. Successful development of aerospace, automotive and aircraft, mechanical engineering, and medicine is impossible without carbon materials or materials derived from them. Carbon nanotubes have unique mechanical properties, offering various applications [1-2]. Carbon nanotubes are a sensitive element of composite reinforcing or functional filler, catalyst and catalyst carrier, hydrogen sorbent, accumulator material for tunnel scanning probes, atomic power and magnetic force microscopy, and gas analyzer nanosensors.

In addition to conventional sources, carbon can also be obtained from petroleum gases and other industrial wastes. The amount of combustion released into the Earth's atmosphere due to oil and gas combustion alone is 0.5 million tons per year [3]. The combustion of petroleum gas leads to thermal pollution of the environment [3-5]. In addition to direct combustion, there are several options for using petroleum gas. Among these options can be distinguished by the direct use of petroleum gas and its processing [6].

There are two main directions for using petroleum gas: 1) as a fuel and 2) as a raw material for petrochemistry [7-9].

In addition, it is possible to organize the production of motor fuel in the fields, the development of the gas-chemical industry and the production of new products from oil and gas raw materials [10-13]. When a gaseous hydrocarbon mixture is catalytically decomposed, carbon nanomaterials and hydrogen are formed. Hydrogen, in turn, is used effectively in the petrochemical and pharmaceutical industries. Hydrogen is an environmentally friendly energy carrier. When hydrogen is compared to other energy sources, its advantages are noticeable. For example, hydrogen is highly efficient and environmentally friendly (harmless to humans and nature). Hydrogen has great potential for future use, especially fueling vehicles and fuel cells. [14].

Developing promising materials for hydrogen storage is one of the most important tasks in improving the hydrogen economy [15-17]. One such effective and attractive way to store hydrogen is to store it in metal hydrides. Hydrides have a high density compared to liquid hydrogen, have a wide range of operating pressures and temperatures, and do not require temperature to store hydrogen. To further improve the storage properties of hydrides, other materials may be added to them, such as transition metals [18], oxides [19], carbon nanotubes [20-21], and other additives.

Creating catalysts with high catalytic activity for producing carbon nanomaterials and hydrogen from carbon compounds is one of the issues that does not lose its relevance today. Therefore, the aim was to create catalysts with high catalytic activity and to study the catalytic activity of this catalyst.

2 Methods

A catalyst containing 15%Ni*5%Co*5%Fe*5%Cu*2%Mo/HSZ was prepared by precipitation of nitrates of the corresponding metals [33-35]. The calculated amount of salts of $Co(NO_3)_2 \cdot 6H_2O$, $Ni(NO_3)_2 \cdot 6H_2O$, $Fe(NO_3)_3 \cdot 9H_2O$, $Cu(NO_3)_2 \cdot 6H_2O$ was dissolved in 200 ml of distilled water and then precipitated with ammonia at pH = 9. The precipitate obtained remained under its own liquid for 30 minutes at room temperature. The precipitate was washed with copious amounts of water to a neutral pH. In a separate beaker, a certain amount of $(NH_4)_2MoO_4$ is dissolved in 20 ml of distilled water; the solution is added to the pre-obtained precipitate, mixed, dried in a muffle furnace at 350°C for 30 minutes and then at 500°C for one hour.

Electron microscopy (SEM) scanning the morphological composition of the samples was performed on a device "JEOL JSM-6390 LA" equipped with a part of energy

dispersive X-ray (EDX) microanalysis. We place the sample on double-sided carbon conductive tape glued to a copper-chrome table. Then we vacuum it in the instrument chamber. Microphotography recording was performed at 5-25 kV working distances and 8-10 mm under accelerating voltage. EDX spectra were recorded at 20 kV at a working distance of 10 mm. The microstructure of the samples was examined by scanning electron microscopy. The JEOL 2100F used an accelerating voltage of 200 kV. The samples were dispersed, processed by ultrasound in methanol, and smeared on a copper wall. The catalysts were preheated and passivated at 400°C for 4 h at 30 ml/min of nitrogen flow. The processed catalysts were also passivated at room temperature after the reaction in the oxygen-argon 2 vol.% O_2/Ar mixture had stopped. We performed the average size of the metal particles and the diameter of the carbon nanotubes in the Image-ProPlus program. We calculated the average size of 500 particles for each catalyst, and 100 carbon nanotubes were processed to measure the average diameter of the carbon nanotubes.

The synthesized catalysts were tested in a flow quartz reactor in the decomposition reactions of hydrocarbons. The process of obtaining nanocarbon from methane can be represented by the following scheme (Fig. 1):
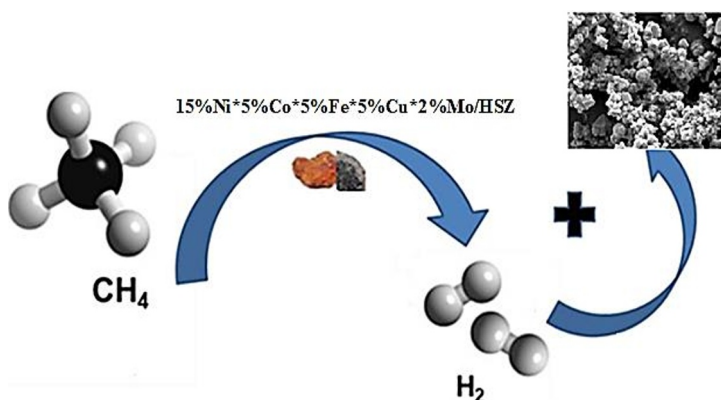

Fig. 1. Schematic diagram of the formation of nanocarbons and hydrogen from methane.

The laboratory device for obtaining nanocarbon is shown in Fig. 2.

Fig. 2. Laboratory device for nanocarbon extraction

3 Results and discussion

Figure 3 shows the kinetic curve of carbon nanotubes growth in a catalyst of 15%Ni*5%Co*5%Fe*5%Cu*2%Mo/HSZ from butadiene-1,3 diluted with hydrogen at a molar ratio of C_4H_6:H_2=1:20 at a temperature of 700 ℃.
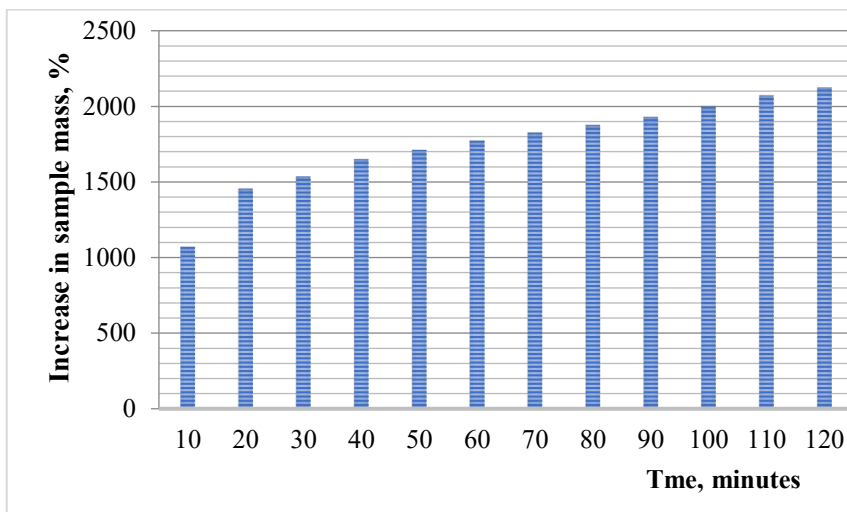

Fig. 3. Kinetic curve of carbon nanotubes growth in a catalyst of 15%Ni*5%Co*5%Fe*5%Cu*2%Mo/HSZ from butadiene-1.3 diluted with hydrogen at a molar ratio of C_4H_6:H_2=1:20 at a temperature of 700℃.

As seen from Fig. 3, the mass of the sample increased by about 22 times. Electron microscopic studies have shown that carbon nanotubes grow directly on the catalyst. After synthesis and functionalization of the carriers in the catalyst of 15%Ni*5%Co*5%Fe*5%Cu*2%Mo/HSZ, the nanocarbons were condensed, their outer diameter remained unchanged and was 10-30 nm (Fig. 4).
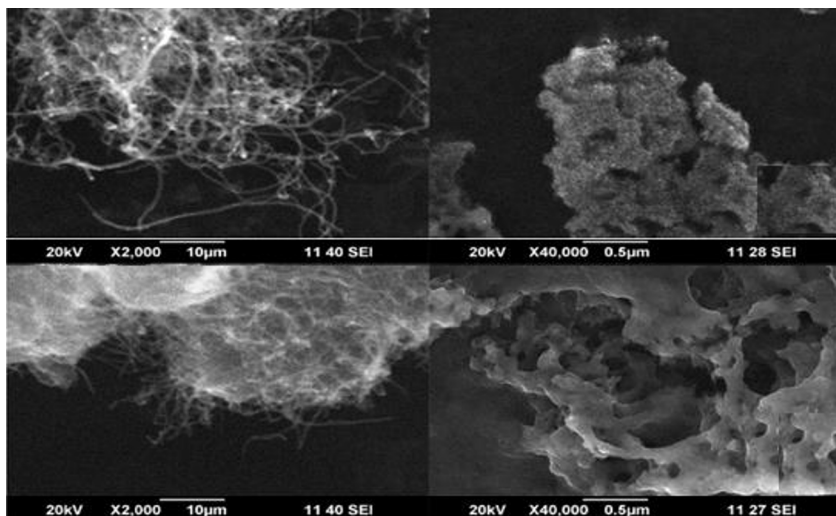

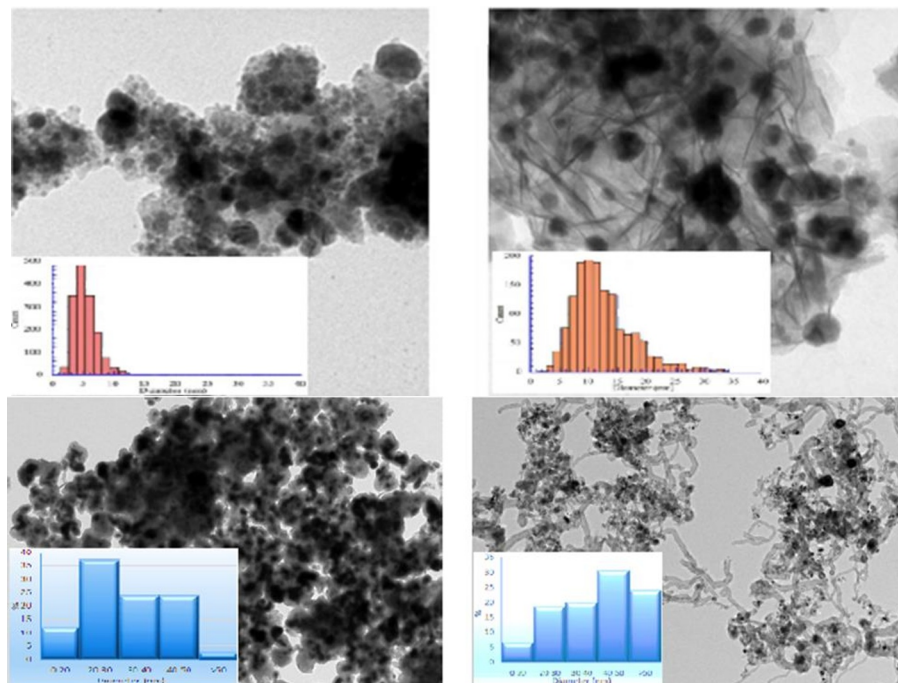**Fig. 4.** SEM image of nanocarbons.

Fig. 5. Electron microscopic photograph of carbon nanotubes in a catalyst of 15%Ni*5%Co*5%Fe*5%Cu*2%Mo/HSZ from butadiene-1,3 diluted with hydrogen at a molar ratio of C_4H_6:H_2=1:20 at a temperature of 700℃.

Carbon nanotubes range in diameter from 5 to 15 nm, depending on the size of the metal particles, and in length from a few microns. The growth of nanotubes is due to the highly dispersed metal particles located at their ends. Larger iron particles are characterized by changes in the diameter of carbon nanotubes during growth. At the beginning of growth, the diameter of such a nanotube is 30 ... 50 nm; however, it decreases to 5 ... 15 nm. In particular, it should be noted that part of the inner cavity of carbon nanotubes is filled with metal (Fig. 5). It is known that the diameter of carbon nanotubes is determined by the size of the metal particles that catalyze their growth. In this case, the diameter of the carbon tubes also changes due to the reduction in the size of these particles. Thus, carbon nanotubes of sufficiently different diameters grow on the catalyst of 15%Ni*5%Co*5%Fe*5%Cu*2%Mo/HSZ.

Reduction experiments were performed in a hydrogen stream to study the final state of a catalyst containing 15%Ni*5%Co*5%Fe*5%Cu*2%Mo/HSZ after complete reduction. A catalyst containing 15%Ni*5%Co*5%Fe*5%Cu*2%Mo/HSZ was studied by X-ray diffraction method after complete reduction in hydrogen for 90 minutes at a temperature of 500, 550, 600℃ (Fig. 6). Reflexes associated with the Fe-Mo alloy were observed on the radiograph. It was found that the grid parameter of the metal iron increased to 2,876 Å. The concentration of molybdenum in solid Fe-Mo solution is 4.4 at.% or 7.5 mass.%. Using the half-width line, we estimated the average particle size of the Fe-Mo alloy formed after the reduction of a catalyst containing 15%Ni*5%Co*5%Fe*5%Cu*2%Mo/HSZ in hydrogen to 30 nm [21-25].
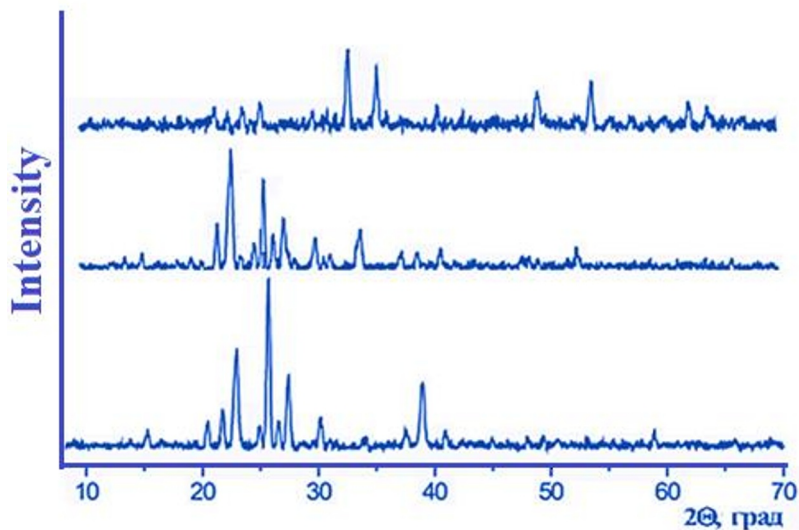
Fig. 6. X-ray of a catalyst containing 15%Ni*5%Co*5%Fe*5%Cu*2%Mo/HSZ after reduction in hydrogen for 90 minutes at a temperature of 500, 550, 600°C.

Consequently, the oxides (MoO_3 and Fe_2O_3) introduced into the catalyst containing 15%Ni*5%Co*5%Fe*5%Cu*2%Mo/HSZ are returned to the metals and subsequently react with each other to form the Fe-Mo alloy. Enrichment with molybdenum oxide significantly changes the catalytic properties of the catalyst containing 15%Ni*5%Co*5%Fe*5%Cu*2%Mo/HSZ (Fig. 7).
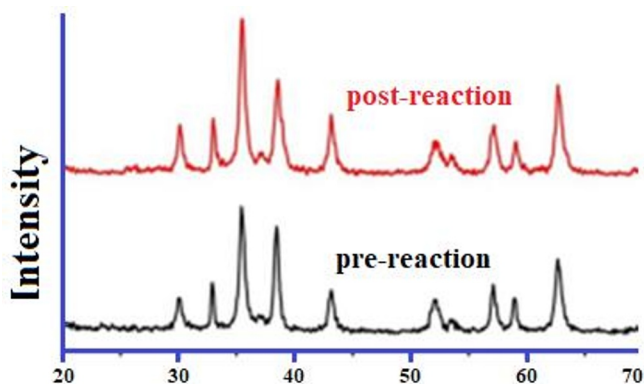

Fig. 7. Pre- and post-reaction radiographs of the catalyst containing 15%Ni*5%Co*5%Fe*5%Cu*2%Mo/HSZ.

Figures 8-11 shows the first segments of the kinetic curves for the formation of carbon nanotubes in catalysts containing 15%Ni*5%Co*5%Fe*5%Cu/HSZ and 15%Ni*5%Co*5%Fe*5%Cu*2%Mo/HSZ at a temperature of 700 °C in butadiene-1,3 diluted with hydrogen in a molar ratio of $C_4H_6:H_2=1:20$.
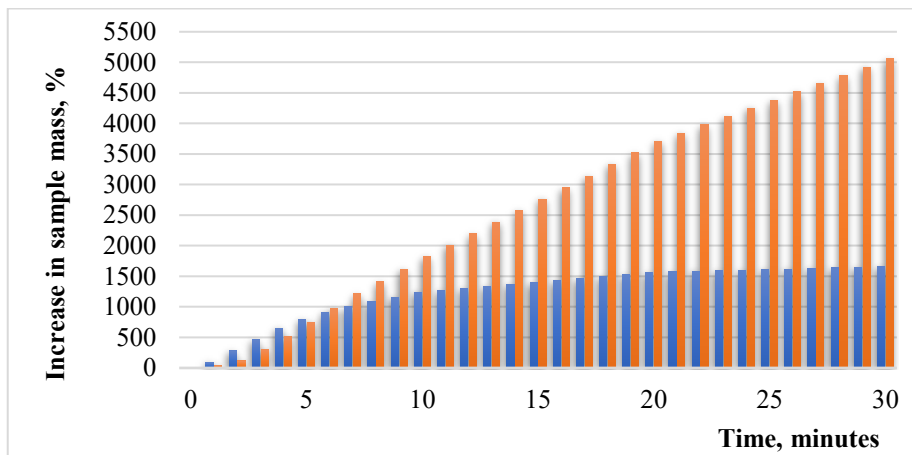
Fig. 8. Kinetic curves for forming carbon nanotubes in various molybdenum-containing catalysts from butadiene-1,3 diluted with hydrogen at a molar ratio of $C_4H_6:H_2=1:20$ at a temperature of 700 °C: 1 is 15%Ni*5%Co*5%Fe*5%Cu/HSZ; 2 is 15%Ni*5%Co*5%Fe*5%Cu*2%Mo/HSZ

The results show that the initial rate of formation of carbon nanotubes in the 15%Ni*5%Co*5%Fe*5%Cu*2%Mo/HSZ catalyst is higher than that of the 15%Ni*5%Co*5%Fe*5%Cu/HSZ-containing catalyst. However, the average size of the Fe particles is larger than the average size of the Fe-Mo alloy particle. Consequently, the addition of molybdenum reduces the rate of formation of carbon nanotubes.

We then mechanochemically and ultrasonically activated the obtained nanocarbon. The results obtained are shown in the following figures.
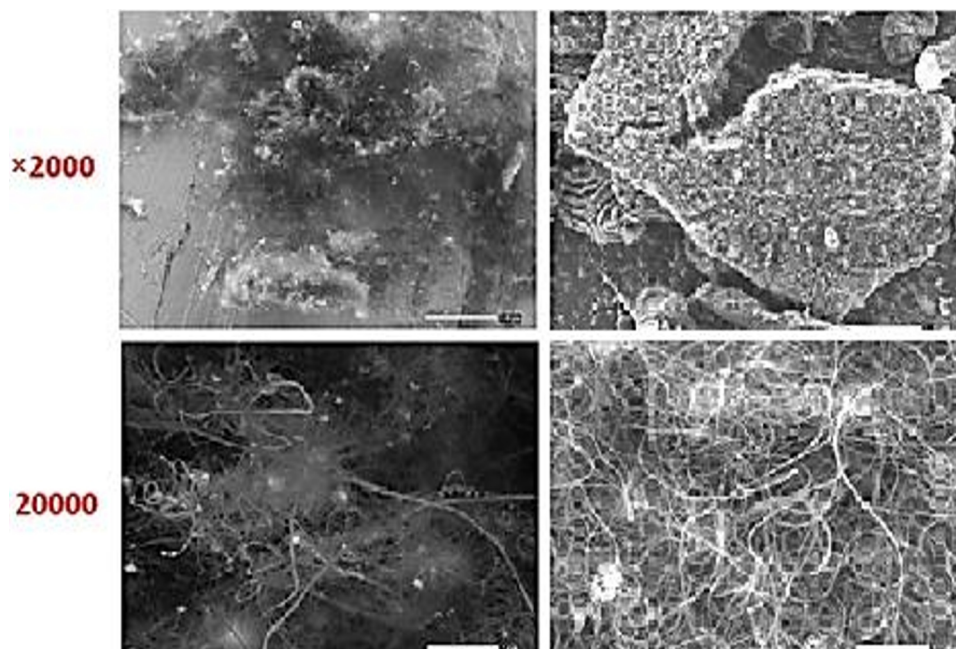

Fig. 9. SEM image of nanocarbons: on the left - before mechanical activation, on the right - 2 minutes after mechanical activation
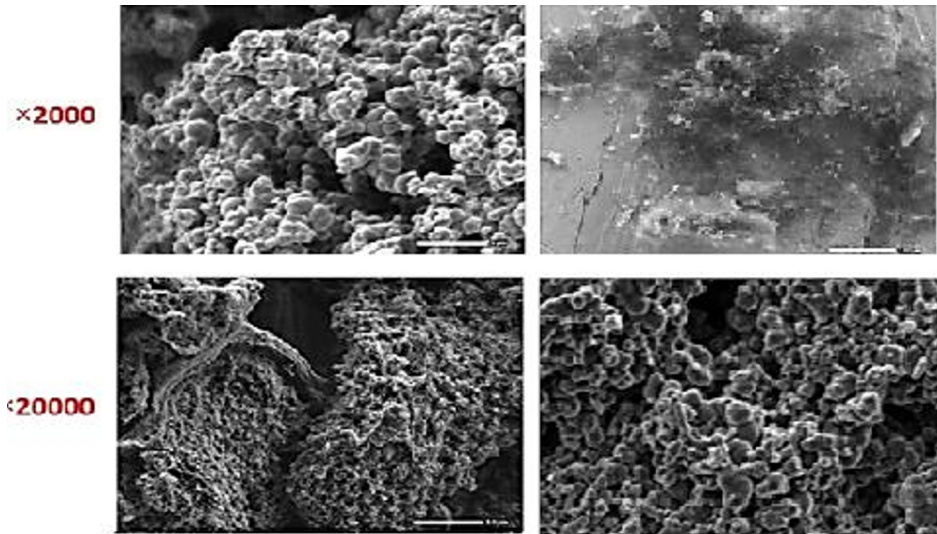
Fig. 10. SEM image of nanocarbons: on the left - after mechano-chemical activation for 5 minutes in isopropanol medium, on the right - after ultrasonic treatment for 5 minutes in isopropanol medium
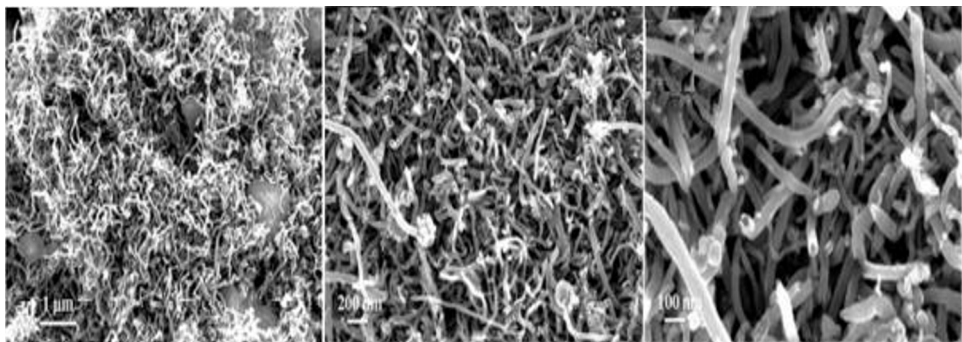

Fig. 11. SEM image of nanogenerate obtained in 15%Ni*5%Co*5%Fe*5%Cu*2%Mo/HSZ catalyst

4 Conclusions

1. The possibilities of obtaining nano carbons from hydrocarbons were studied in a catalyst containing 15%Ni*5%Co*5%Fe*5%Cu*2%Mo/HSZ, and the texture characteristics of the catalyst used and the obtained nano carbon were studied.

2. A catalyst containing 15%Ni*5%Co*5%Fe*5%Cu*2%Mo/HSZ is prepared by precipitation of nitrates of the corresponding metals.

3. After the synthesis and functionalization of the carriers in the 15%Ni*5%Co*5%Fe*5%Cu*2%Mo/HSZ catalyst, the nano carbon were condensed, and their outer diameter remained unchanged and was 10-30 nm. Carbon nanotubes range in diameter from 5 to 15 nm, depending on the size of the metal particles, and in length from a few microns.

4. The growth of nanotubes is due to metal particles with high dispersion located at their ends. Larger iron particles are characterized by changes in the diameter of carbon nanotubes during growth. At the beginning of growth, the diameter of such a nanotube is 30...50 nm; however, then it decreases to 5...15 nm.

References

1. M.Meyyappan, H.Partridge. Carbon nanotube based nanotechnology - Opportunities and challenges // 15th AIAA Computational Fluid Dynamics Conference, Issue: 2001.

2. N.Choudhary, W.Choi. Graphene Synthesis and Applications // Handbook of Carbon Nano Materials World Scientific Series on Carbon Nanoscience. 2015, on.p.1-49.

3. Carmen-Mihaela Tîlmaciu, May C.Morris. Carbon nanotube biosensors // Frontiers in Chemistry. Issue: 2015

4. O.O.Ayodele, M.A.Awotunde, M.B.Shongwe, A.O.Adegbenjo, B.J.Babalola, A.T.Olanipekun, P.A.Olubambi. Carbon nanotube-reinforced intermetallic matrix composites: processing challenges, consolidation, and mechanical properties // The International Journal of Advanced Manufacturing Technology, 2019, Issue: 9-12, on.p.3803-3820

5. Y.Hanein. Carbon nanotube integration into MEMS devices // Physica status solidi (b), 2010, Issue 11-12, on.p.2635-2640

6. V.N.Bashkin, R.V.Galiulin. Geoecological Risks in the Gas Industry // Environmental Pollution Geoecological Risk Management in Polar Areas. Issue: 2019, on.p.35-46

7. E.Voskresenskaya, L.Vorona-Slivinskaya, D.Mokhorov, A.Ponomarenko Legal regulation of environmental protection and ensuring environmental safety when using underground resources at regional and local levels // MATEC Web of Conferences. Issue: 2019.

8. Y.Kopylov, L.Vstavskaya, A.Mazgarov, M.Gibadukov, V.Gorbunov. Light hydrocarbon feedstock for petrochemical industry (review) // Petroleum Chemistry U.S.S.R. 1990, Issue 2, on.p.116-130.

9. L.V.Eder, I.V.Provornaya, I.V.Filimonova. "Problems of Rational Use of Associated Petroleum Gas in Russia // Geography and Natural Resources, 2019, Issue 1, on.p.9-14.

10. Li Na Zheng, Zhi Zhang, Jing Ni Xiao, Hong Wang. Environmental Risk Assessment of Petrochemical Project // Advanced Materials Research. Issue: 2013, on.p.1130-1133.

11. S.M.Aldoshin. Achievements and innovation prospects of chemical science // Herald of the Russian Academy of Sciences, 2012, Issue 3, on.p.143-157.

12. Chun Jin, Wei Li, Yasi Chen, Rui Li, Jiabin Huo, Qinyu He, Yinzhen Wang. Efficient Photocatalytic Degradation and Adsorption of Tetracycline over Type-II Heterojunctions Consisting of ZnO Nanorods and K-Doped Exfoliated g-C3N4 Nanosheets // Industrial & Engineering Chemistry Research, 2020, Issue 7, on.p.2860-2873.

13. Zhiqiang Chen,Kevin Magniez, Marin Duchemin, Nikki Stanford, Arun T. Ambujakshan, Adam Taylor ,Cynthia S. Wong, Yan Zhao, Xiujuan J. Dai. Rapid Formation of Diamond-Like Nano-Carbons in a Gas Bubble Discharge in Liquid Ethanol // Plasma Chemistry and Plasma Processing, 2017, Issue 1, on.p.75-87.

14. A.L.Ortiz, M.J.M.Zaragoza, V.Collins-Martínez. Hydrogen production research in Mexico: A review // International journal: Hydrogen Energy 2016, 41, on.p.2363-2379.

15. N.Armaroli, V.Balzani. The hydrogen issue // ChemSusChem, 2011, 4, on.p.21-36.

16. E.Rivard, M.Trudeau, K.Zaghib. Hydrogen storage for mobility: A review. Materials 2019, 12.

17. N.Hanada, T.Ichikawa, H.Fujii. Catalytic effect of nanoparticle 3d-transition metals on hydrogen storage properties in magnesium hydride MgH_2 prepared by mechanical

milling // Journal Phys.Chem.B 2005, 109, on.p.7188-7194.

18. M.G.Shelyapina, D.Fruchart. Role of transition elements in stability of magnesium hydride: A review of theoretical studies. Solid State Phenom, 2011, 170, on.p.227–231.

19. A.Patah, A.Takasaki, J.S.Szmyd. Synergetic effect of oxides on hydrogen reaction kinetics of magnesium hydride. Mater. Sci. Forum 2007, 561, on.p.1605–1608.

20. K.S.Jung, E.Y.Lee, K.S.Lee. Catalytic effects of metal oxide on hydrogen absorption of magnesium metal hydride // Journal. Alloy. Compd. 2006, 421, on.p.179–184.

21. R.K.Pandyan, S.Seenithurai, S.V.Kumar, M.Mahendran. Magnesium Hydride Doped on Single-Walled Carbon Nanotubes for Hydrogen Adsorption // Fuller. Nanotube. Carbon Nanostruct, 2015, 23, on.p.175–180.

22. C.Z.Wu, P.Wang, X.Yao, C.Liu, D.M.Chen, G.Q.Lu, H.M.Cheng. Effect of carbon/noncarbon addition on hydrogen storage behaviors of magnesium hydride // J. Alloy. Compd. 2006, 414, on.p.259–264.

23. C.Wu, P.Wang, X.Yao, C.Liu, D.Chen, G.Q.Lu, H.Cheng. Effects of SWNT and metallic catalyst on hydrogen absorption/desorption performance of MgH_2 // J. Phys. Chem. B 2005, 109, on.p.2217–2221.

24. I.I.Mamadoliev, N.I.Fayzullaev, K.M.Khalikov, Synthesis of high silicon of zeolites and their sorption properties // International Journal of Control and Automation, 2020, 13(2), on.p.703–709**.**

25. I.I.Mamadoliev, N.I.Fayzullaev. Optimization of the activation conditions of high silicon zeolite. International Journal of Advanced Science and Technology, 2020, 29(3), on.p.6807–6813